Available online at www.sciencedirect.com
ScienceDirect
Dyes and Pigments 76 (2008) 187–194
DYES and PIGMENTS
www.elsevier.com/locate/dyepig

Decolorization of Procion Red MX-5B in electrocoagulation (EC), UV/TiO_2 and ozone-related systems

Chung-Hsin Wu [a], Chung-Liang Chang [b], Chao-Yin Kuo [c,*]

[a] Department of Environmental Engineering, Da-Yeh University, 112, Shan-Jiau Road, Da-Tsuen, Chang-Hua, Taiwan, ROC
[b] Department of Environmental Engineering and Health, Yuanpei University of Science and Technology, 306 Yuanpei Street, Hsinchu, Taiwan, ROC
[c] Department of Safety Health and Environmental Engineering, National Yunlin University of Science and Technology, 123, Sec. 3, University Road, Touliu, Yunlin 640, Taiwan, ROC

Received 17 March 2006; received in revised form 23 May 2006; accepted 16 August 2006
Available online 11 October 2006

Abstract

This investigation assessed the decolorization efficiency of Procion Red MX-5B in electrocoagulation (EC), UV/TiO_2 and ozone-related systems. The effectiveness of energy input was also determined. The decolorization rate constants of these EC, UV/TiO_2 and ozone-related systems fitted pseudo-first-order kinetics and the values were in the order O_3 (24 W) > O_3 (16 W) > O_3 (16 W)/EC (8 W) > UV/TiO_2/O_3 (8 W)/EC (8 W) > O_3 (10 W) > UV/O_3 (8 W)/EC (8 W) > UV/O_3 (8 W) > O_3 (8 W) > UV/TiO_2/O_3 (8 W) > O_3 (8 W)/EC (8 W) > O_3 (4 W)/EC (4 W) > UV/TiO_2/EC (8 W) > UV/TiO_2 > UV/EC (8 W) > EC (8 W). The decolorization rate constants increased with the total power input. Additionally, the decolorization efficiency could be promoted by combining UV with O_3, UV with EC, EC with UV/TiO_2 and EC with UV/O_3. This study reveals that combining EC with UV/TiO_2 or UV/O_3 can trigger a Fenton or Fenton-like reaction, which accelerates the rate of decolorization. The solution pH of O_3, UV/O_3 and UV/TiO_2 systems declined during decolorization; in contrast, the pH increased to 7.4 in the UV/EC system. The effective energy consumption constant did not increase with the total power input and reached maximum at a total power input of approximately 10–16 W.
© 2006 Elsevier Ltd. All rights reserved.

Keywords: Decolorization; Energy consumption; Procion Red MX-5B; Electrocoagulation; UV; TiO_2; O_3

1. Introduction

Wastewater from the textile dyeing industry has a high or low pH, high temperature and a high concentration of coloring material. Numerous dyes represent environmental hazards owing to their toxicity. Azo dyes are the most extensively utilized dyes and are normally major pollutants in dye effluents. Treatment costs are very large for most textile factories, explaining the need to develop more efficient and economic methods, which consume less chemical and energy. Conventional treatments of dye effluents include biological oxidation and adsorption. Although less expensive than other approaches, biological treatment is ineffective for decolorization because the dyes are toxic. Adsorption onto activated carbon transfers most of the contaminant from the wastewater to the solid phase. This method therefore requires further disposal of the sludge. Electrocoagulation (EC) is regarded as a potentially effective method for treating textile wastewater with high decolorization efficiency and with the formation of relatively little sludge. Several researchers have reported treatments of dye wastewater based on the EC method [1–5]. EC applies an electric current to produce metal ions in solution. Metal ions can react with the OH^- ions formed at the cathode during the evolution of hydrogen gas, to yield insoluble hydroxides that sorb pollutants out of the solution. The EC process can be summarized as follows (Eqs. (1) and (2)) [1].

* Corresponding author. Fax: +886 5 5334958.
E-mail address: kuocyr@ms35.hinet.net (C.-Y. Kuo).

0143-7208/$ - see front matter © 2006 Elsevier Ltd. All rights reserved.
doi:10.1016/j.dyepig.2006.08.017

At the anode,

$$M \rightarrow M^{n+} + ne^{-} \quad (1)$$

At the cathode,

$$nH_2O + ne^{-} \rightarrow n/2\,H_2 + nOH^{-} \quad (2)$$

where M is the anode material and n is the number of electrons that are involved in the reaction. The insoluble metal hydroxides react with pollutants by surface complexation, coagulation or electrostatic attraction. Previous studies had established that the decolorization efficiency is proportional to the current density [1–5], the number of electrodes [4] and the concentration of the electrolyte [2,4] but not to the gap between the electrodes [1,2]. Kim et al. [1] demonstrated that the power consumption of EC increased with the current density and the concentration of the electrolyte but fell as the number of pairs of electrodes increased.

Advanced oxidation processes (AOPs) are alternative approaches for decolorizing and reducing recalcitrant wastewater loads from textile companies. Significant progress has been made in the development of AOPs for textile effluent in recent years, especially in TiO_2 [6–13] and ozone-related processes [12–17]. AOPs involve primarily the generation of a very powerful and non-selective oxidizing agent, the hydroxyl radical (OH•), to destroy hazardous pollutants. In UV/TiO_2-related systems, TiO_2 particles absorb UV energy that is greater than the TiO_2 band gap and form a pair of electron and hole in conduction band and valence band. The positive holes can oxidize water molecules to hydroxyl radicals and the negative electrons reduce molecular oxygen to yield superoxide radical anions (O_2^{-}•). The positive holes, hydroxyl radicals and superoxide radical anions are the dominant oxidizing species in UV/TiO_2 systems. However, the rapid unfavorable recombination of photoproduced electrons and holes in TiO_2 considerably reduces photocatalytic efficiency. The effect of the form of TiO_2 [11,18], TiO_2 loading [7,11], UV intensity [7], UV irradiation time [9,13], solution pH [7,10,11], substrate concentration [11,13] and the presence of different electron acceptors [9,11] in UV/TiO_2-related systems has been extensively investigated. The degradation efficiency typically increases with the UV intensity and irradiation time, the concentration of TiO_2 and the presence of electron acceptors, but is inhibited by an increase in the initial substrate concentration.

Ozonation may be a promising method for decolorization since ozonation can remove color and degrade organics in one step; moreover, no sludge remains in the treated effluent. Ozone oxidizes organics via two possible degradation routes: (i) at basic pH, it rapidly decomposes to yield hydroxyl and other radical species in solution according to Eqs. (3)–(5), and (ii) at acidic pH, ozone is stable and can react directly with organic substrates [19]. UV radiation can decompose ozone in water, generating highly reactive hydroxyl radicals [17]. The hydroxyl radicals are known to be the most powerful oxidizing agents and oxidize organics faster than ozone itself. Ozone has an oxidation potential of 2.07 V, whereas the OH radical has an oxidation potential of 2.80 V; notably, direct oxidation is slower than radical oxidation. The effects of dye concentration [13,20], ozone dose [20,21], pH [12,13,20], the presence or absence of UV [13,17] and UV intensity [17] have been evaluated. The results of these works all indicate that the decolorization efficiency increases with ozone dose, pH and UV intensity, and declines with increasing dye concentration.

$$O_3 + OH^{-} \rightarrow O_3^{-}\bullet + OH\bullet \quad (3)$$

$$O_3^{-}\bullet \rightarrow O^{-}\bullet + O_2 \quad (4)$$

$$O^{-}\bullet + H^{+} \rightarrow OH\bullet \quad (5)$$

The factors that influence dye decolorization in EC, UV/TiO_2 and ozone-related systems have been investigated in several works. However, comparisons of the amounts of energy consumed by these systems are few. Additionally, the effects of combining these methods on dye decolorization and energy consumption have not been examined. Therefore, in this study, Procion Red MX-5B was selected as a parent compound and decolorized with various total power inputs (8, 10, 16 and 24 W). The goals of this study are to compare the decolorization efficiencies and energy consumptions of EC, UV/EC, UV/TiO_2, ozone, UV/ozone, ozone/EC, UV/TiO_2/ozone, UV/TiO_2/EC, UV/ozone/EC and UV/TiO_2/O_3/EC systems. The decolorization rate and effective energy consumption constants were evaluated to identify the appropriate operating system.

2. Materials and methods

2.1. Materials

The parent compound, Procion Red MX-5B, purchased from Aldrich Chemical Company, was used without further purification. The formula, molecular weight and maximum light absorption wavelength (λ_{max}) of Procion Red MX-5B were $C_{19}H_{10}Cl_2N_6Na_2O_7S_2$, 615 g/mol and 538 nm, respectively. TiO_2 was obtained from Degussa P-25 and utilized directly without treatment. The water was deionized and doubly distilled with MINIQ. One pair of Fe plates (outer diameter = 13.7 cm and inner diameter = 4.2 cm) was used as electrodes in EC-related systems and the electrodes were connected to a DC power supply. The total effective electrode area was 133.6 cm^2; the gap between the anode and the cathode was set to 0.4 cm, and the current density was maintained at 1.5 mA/cm^2. In ozone-related systems, a dielectric barrier discharge (DBD) reactor was adopted to generate ozone. A stainless steel wire (5.0 mm diameter) was suspended as an inner electrode along the axis of a Pyrex-glass tube (inner diameter 20.0 mm). The effective length of the DBD reactor was 137 mm. Glass pellets with a diameter of 5 mm were used as packing material, and placed in the plasma region between the two electrodes. A high voltage was applied to the inner electrodes. The DBD reactor consumed various powers (8, 10, 16 and 24 W) in pure oxygen at a flow rate of 500 mL/min. The schematic diagram of the ozone generator and the photoreactor presented herein is same as that of Wu and Chang [13].

2.2. Decolorization experiments

Vaporization, adsorption (in TiO_2 suspension) and direct photolysis were performed to compare the decolorization efficiency of Procion Red MX-5B across all of these reactions. Decolorization experiments were undertaken in a 3 L hollow cylindrical glass reactor. The inner tube was made of quartz with an 8 W, 365 nm UV-lamp (Philips) placed inside it as the source of irradiation. The intensity of the UV-lamp was 4.32 mW/cm^2. In UV/TiO_2-related systems, the concentration of TiO_2 was 0.5 g/L in all experiments. All the systems were stirred continuously at 300 rpm. The Procion Red MX-5B concentration was 20 ppm in all experiments. A 15 mL aliquot was withdrawn from the photoreactor at pre-specified intervals. The suspended solids in UV/TiO_2 and EC-related systems were separated by centrifugation at 5000 rpm for 10 min, and then filtered through a 0.22 μm filter (Millipore). Decolorization of Procion Red MX-5B was detected using a spectrophotometer (HACH DR/4000U) at 538 nm and the concentration was determined from the calibration curve using Beer–Lambert's law. The decolorization efficiency was calculated from the difference between the dye concentrations before and after experiment. In ozone-related systems, ozone was aerated into the reactor at a flow rate of 500 mL/min. For the measurement of ozone concentration, ozone was pumped into D.I. water for 10 min and then the ozone concentration in aqueous solution was measured using a fast-responding ozone probe (EMERSON, 499A OZ). In UV/TiO_2 and EC-related systems, the same flow rate (500 mL/min) of air was input into the reactor to maintain similar experimental conditions.

3. Results and discussion

3.1. Decolorization efficiency of ozone and UV/ozone systems

This work applied pure oxygen as the source gas to generate ozone to decolorize Procion Red MX-5B under various power inputs. Fig. 1 displays the dye decolorization efficiency of these systems. In ozone-only systems, the decolorization ratios in 3 min were 43, 57, 72 and 95% at power inputs of 8, 10, 16 and 24 W, respectively (Fig. 1). The concentrations of ozone dissolved by the ozone generator at power inputs of 8, 10, 16 and 24 W were measured to be 3.1, 5.0, 9.1 and 10.4 mg/L, respectively. The solubility of ozone depends on the temperature of water and the concentration of ozone in the gas phase. The concentration of ozone in a clean water system at pH 7 at a gas flow rate of 1–3 L/min was 8.6–11.0 mg/L [22]. The ozone concentration in this work seemed to reach saturation at an input power of 16 W, so the ozone concentration was insignificantly higher at a power input of 24 W. The experimental results revealed that the higher input power generated a higher ozone concentration, so a higher decolorization efficiency was observed. Konsowa [20] and Koch et al. [21] also showed that the decolorization efficiency increased with the ozone concentration. Plotting $\ln(C_o/C)$ versus time yields the decolorization rate constant (k_a). The k_a values of photocatalytic systems

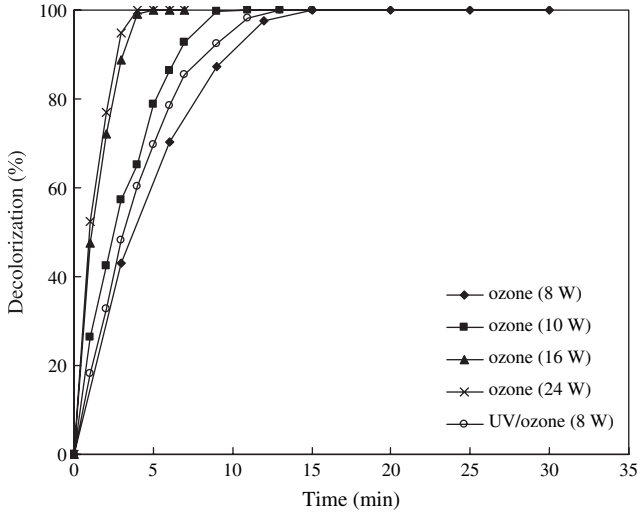

Fig. 1. Decolorization efficiency of ozone and UV/ozone systems (Procion Red MX-5B = 20 ppm, UV = 8 W, ozone flow rate = 500 mL/min and T = 25 °C).

exhibit pseudo-first-order kinetics, and numerous works have demonstrated that dye decolorization rates can generally be approximated as pseudo-first-order kinetics [8,13,23]. The decolorization efficiencies of various photocatalytic systems can thus be compared in terms of the k_a values (Table 1).

The k_a value of UV/O_3 (8 W) (17.94 h^{-1}) exceeded that of O_3 (8 W) (15.92 h^{-1}). Combining O_3 with UV promotes the degradation of dyes by the direct and indirect production of hydroxyl radicals following O_3 decomposition and H_2O_2 formation, respectively (Eqs. (6)–(9)) [14]:

$$O_3 + h\nu \rightarrow O_2 + O \quad (6)$$

$$O + H_2O \rightarrow OH^{\bullet} + OH^{\bullet} \quad (7)$$

$$O + H_2O \rightarrow H_2O_2 \quad (8)$$

$$H_2O_2 + h\nu \rightarrow OH^{\bullet} + OH^{\bullet} \quad (9)$$

UV radiation enhances ozone decomposition, yielding more free OH radicals and thereby increasing the decolorization rate. Various studies have also established that UV promotes ozone decolorization [14,17].

3.2. Decolorization efficiency of EC, UV/EC, UV/TiO_2 and UV/TiO_2/EC systems

Fig. 2 presents the decolorization efficiency of EC, UV/EC, UV/TiO_2 and UV/TiO_2/EC systems. The reaction rate constants of these systems followed the trend UV/TiO_2/EC (0.89 h^{-1}) > UV/TiO_2 (0.35 h^{-1}) > UV/EC (0.26 h^{-1}) ≧ EC (0.22 h^{-1}) (Table 1). EC with iron electrodes involves the following reactions (Eqs. (10)–(13)) [24]:

$$\text{Anode}: 4Fe_{(s)} \rightarrow 4Fe^{2+}_{(aq)} + 8e^- \quad (10)$$

$$4Fe^{2+}_{(aq)} + 10H_2O_{(l)} + O_{2(g)} \rightarrow 4Fe(OH)_{3(s)} + 8H^+_{(aq)} \quad (11)$$

Table 1
Reaction rate constants (k_a, h^{-1}) and effective energy consumption constants (k_b, kJ^{-1})

Systems	Reaction rate constant		Effective energy consumption constant	
	k_a	r^2	k_b	r^2
8 W				
O_3 (8 W)	15.92	0.935	27.35	0.989
UV/TiO_2	0.35	0.994	0.74	0.994
EC (8 W)	0.22	0.998	0.46	0.998
O_3 (4 W)/EC (4 W)	4.15	0.997	8.65	0.997
10 W				
O_3 (10 W)	19.83	0.960	30.58	0.979
16 W				
O_3 (16 W)	41.95	0.990	43.69	0.990
UV/O_3 (8 W)	17.94 (0.11)	0.938	16.57	0.979
O_3 (8 W)/EC (8 W)	10.03 (−0.61)	0.986	11.68	0.949
UV/TiO_2/O_3 (8 W)	14.68 (−0.25)	0.909	15.29	0.909
UV/EC (8 W)	0.26 (0.15)	0.998	0.26	0.998
UV/TiO_2/EC (8 W)	0.89 (0.31)	0.999	0.92	0.999
24 W				
O_3 (24 W)	53.61	0.960	30.74	1.000
O_3 (16 W)/EC (8 W)	22.42 (−0.88)	0.946	15.56	0.946
UV/O_3 (8 W)/EC (8 W)	18.89 (0.04)	0.933	13.12	0.933
UV/TiO_2/O_3 (8 W)/EC (8 W)	20.04 (0.07)	0.963	13.91	0.963

UV power is 8 W in all systems.
() Presents the synergy coefficient and the

$$\text{Synergy coefficient} = \frac{k_{a(\text{system A+system B+system C})} - k_{a(\text{system A+system B})} - k_{a(\text{system A+system C})}}{k_{a(\text{system A+system B+system C})}}$$

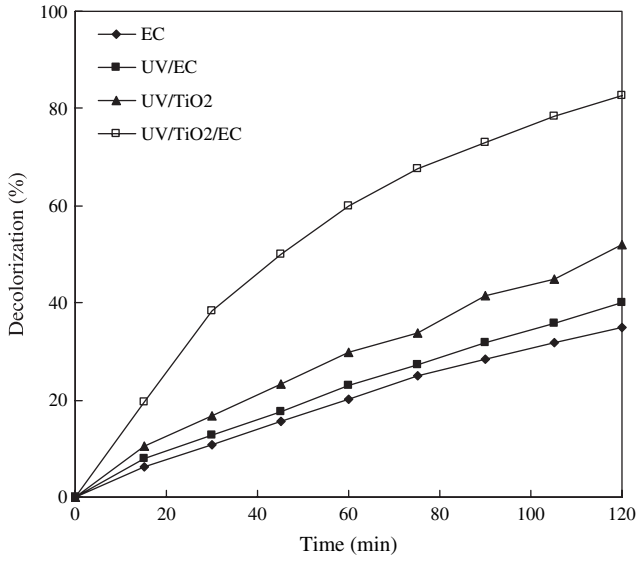

Fig. 2. Decolorization efficiency of EC, UV/EC, UV/TiO_2 and UV/TiO_2/EC systems (Procion Red MX-5B = 20 ppm, UV = 8 W, TiO_2 = 0.5 g/L, EC = 0.2 A, current density = 1.5 mA/cm^2 and T = 25 °C).

$$\text{Cathode}: 8H^+_{(aq)} + 8e^- \rightarrow 4H_{2(g)} \quad (12)$$

$$\text{Overall}: 4Fe_{(s)} + 10H_2O_{(l)} + O_{2(g)} \rightarrow 4Fe(OH)_{3(s)} + 4H_{2(g)} \quad (13)$$

$Fe(OH)_3$ can remove dye from wastewater by the complexation, electrostatic attraction and coagulation. In this work, the EC-related systems are completely mixed using aerating air (500 mL/min); hence, experiments are performed under aerobic conditions and the following reaction (Eq. (14)) can be conducted

$$Fe^{2+} \rightarrow Fe^{3+} + e^- \quad (14)$$

$Fe(OH)^{2+}$ is the predominant Fe^{3+}-hydroxy species in solution at pH 2.5–5.5 and $Fe(OH)^{2+}$ easily absorbs light (300–400 nm) to generate hydroxyl radicals (Eq. (15)) [25].

$$Fe(OH)^{2+} + h\nu \rightarrow Fe^{2+} + OH\bullet \quad (15)$$

Other Fe^{3+}-complexes, such as $Fe(OH)^+_2$, which dominate at pH > 5.5, are less photo-reactive. Moreover, Fe^{2+} does not absorb light above 300 nm and so is not expected to undergo photolysis under the experimental conditions used herein [25]. During the reaction, the pH increases from 6.1 to 7.4 in the UV/EC system, so $Fe(OH)^+_2$ might be the predominant species. Hence, the enhancement of UV in UV/EC system is very limited and proves the result UV/EC (0.26 h^{-1}) ≧ EC (0.22 h^{-1}).

Konstantinou and Albanis [23] summarized the degradation of dye in UV/TiO_2 as follows (Eqs. (16)–(23)):

$$TiO_2 + h\nu \rightarrow TiO_2(e_{CB-} + h_{VB+}) \quad (16)$$

$$TiO_2(h_{VB+}) + H_2O \rightarrow TiO_2 + H^+ + OH\bullet \quad (17)$$

$$TiO_2(h_{VB+}) + OH^- \rightarrow TiO_2 + OH\bullet \quad (18)$$

$$TiO_2(e_{CB-}) + O_2 \rightarrow TiO_2 + O_2^-\bullet \quad (19)$$

$$O_2^-\bullet + H^+ \rightarrow HO_2\bullet \quad (20)$$

$$\text{Dye} + OH\bullet \rightarrow \text{degradation products} \quad (21)$$

$$\text{Dye} + h_{VB+} \rightarrow \text{oxidation products} \quad (22)$$

$$\text{Dye} + e_{CB-} \rightarrow \text{reduction products} \quad (23)$$

Qu et al. [26] further suggested that the mechanism of UV/TiO_2 might have occurred from Eq. (20), then to Eqs. (24)–(26).

$$e_{CB-} + H^+ + O_2^-\bullet \rightarrow HO_2^- \quad (24)$$

$$HO_2^- + H^+ \rightarrow H_2O_2 \quad (25)$$

$$H_2O_2 + e_{CB-} \rightarrow OH^- + OH\bullet \quad (26)$$

Chen et al. [27] provided similar concept equations (Eqs. (27) and (28)) for the UV/TiO_2 system.

$$2HO_2^{\bullet} \rightarrow O_2 + H_2O_2 \quad (27)$$

$$H_2O_2 + O_2^{-\bullet} \rightarrow O_2 + OH^- + OH^{\bullet} \quad (28)$$

These investigations suggest that hydroxyl radicals (OH•), superoxide radical anions (O_2^{-}•), hydrodioxyl radicals (HO_2•) and photogenerated holes (h_{VB+}) are the primary oxidizing species in the UV/TiO_2 system. Furthermore, H_2O_2 was generated in an UV/TiO_2 reaction (Eqs. (25) and (27)). Fe^{2+} and Fe^{3+} were generated in the EC system (Eqs. (10) and (14)), so combining UV/TiO_2 with EC may cause a Fenton or Fenton-like reaction and accelerate decolorization. Chen et al. [9] stated that H_2O_2 plays an important role in reducing electron/hole recombination and promoting the photocatalytic activity of TiO_2. The presence of Fe^{2+} and Fe^{3+} may increase photocatalytic activity, either by scavenging electrons, reducing the recombination of charges, favoring the formation of hydroxyl radicals, or by intermediate Fenton reactions. Hence, UV/TiO_2 and EC combination is a more powerful method than UV/TiO_2 or EC for wastewater treatment.

Fig. 3 shows UV–vis spectral changes of Procion Red MX-5B in various systems. Procion Red MX-5B had a major absorption peak at 538 nm, which fell after 15 min of photocatalytic reaction. The main absorption peak declined, but some intermediates may have been generated following the photocatalytic reaction, but this work did not further elucidate this possibility. In the air inlet for ozone generation systems, the concentrations of dissolved ozone at power inputs of 8, 10, 16 and 24 W were 1.3, 2.2, 4.1 and 4.9 mg/L, respectively, and these dissolved ozone concentrations were lower than those of pure oxygen used as the source gas to generate ozone at the corresponding power inputs; therefore, the decolorization efficiency was low.

Fig. 4 plots the variation of pH in UV/TiO_2, ozone, UV/ozone and UV/EC systems. Except for UV/EC, the pH of all systems declined during the reaction. In an UV/EC system, the cathode releases hydroxide ions according to Eq. (2),

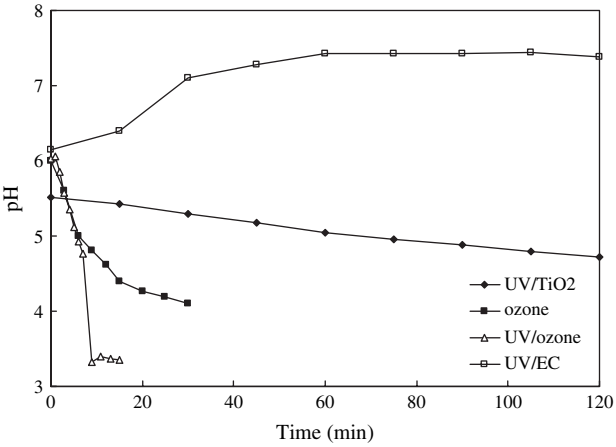

Fig. 4. Variation of pH among various systems (Procion Red MX-5B = 20 ppm, ozone flow rate = 500 mL/min, TiO_2 = 0.5 g/L, EC = 0.2 A, current density = 1.5 mA/cm^2 and T = 25 °C).

increasing the pH. The pH increased from 6.1 to 7.4 in a manner similar to that identified by Daneshvar et al. [2], who used the EC to neutralize the solution. In contrast, photogenerated holes in the UV/TiO_2 system react with water molecules to release hydrogen ions, according to Eq. (17), reducing pH. The most important contribution of the decrease in pH during decolorization is the generation of acidic intermediates or final-products. The major intermediates of azo dyes in an UV/TiO_2 system were organic aromatic and aliphatic carboxylic acids [8,28], which reduce pH. Koch et al. [21] degraded azo dye in an ozone system and identified the main oxidation products as sulfate, nitrate, formate and oxalate. These products were responsible for the decline in pH.

3.3. Decolorization efficiency in conjunctive EC, UV/TiO_2 and ozone-related systems

Fig. 5 depicts the decolorization efficiency of all ozone-related systems at an ozone generator power input of 8 W. The

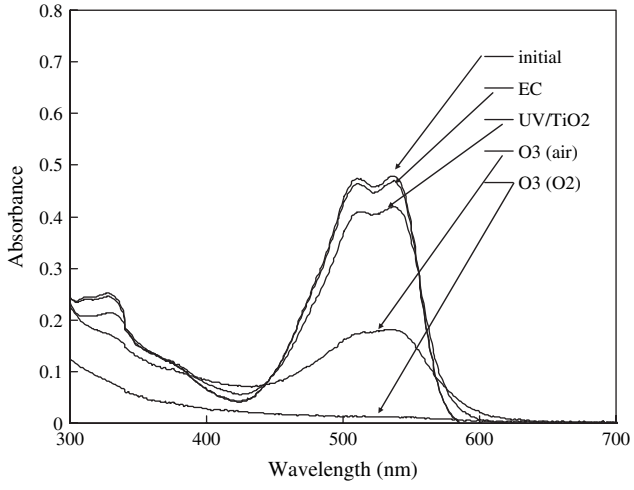

Fig. 3. UV–vis spectral changes of Procion Red MX-5B (20 ppm) in various systems (ozone flow rate = 500 mL/min, reaction time = 15 min, EC = 0.2 A, current density = 1.5 mA/cm^2 and T = 25 °C).

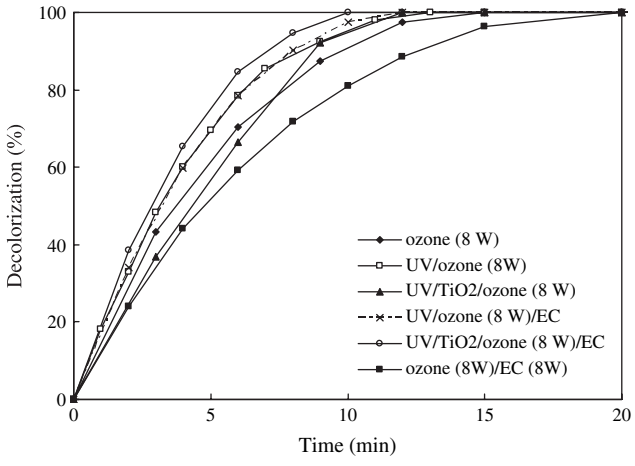

Fig. 5. Decolorization efficiency of all ozone (8 W)-related systems (Procion Red MX-5B = 20 ppm, UV = 8 W, ozone flow rate = 500 mL/min, TiO_2 = 0.5 g/L, EC = 0.2 A, current density = 1.5 mA/cm^2 and T = 25 °C).

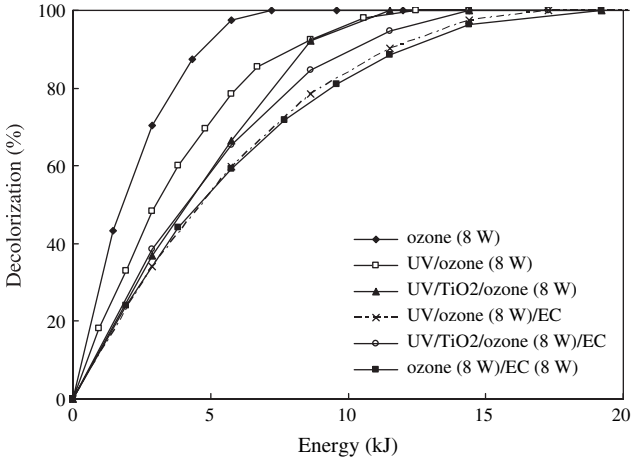

Fig. 6. Relationship between decolorization efficiency and total energy consumption for all ozone (8 W)-related systems (Procion Red MX-5B = 20 ppm, UV = 8 W, ozone flow rate = 500 mL/min, TiO_2 = 0.5 g/L, EC = 0.2 A, current density = 1.5 mA/cm^2 and T = 25 °C).

reaction rate constants follow the order UV/TiO_2/O_3 (8 W)/EC (8 W) > UV/O_3 (8 W)/EC (8 W) > UV/O_3 (8 W) > O_3 (8 W) > UV/TiO_2/O_3 (8 W) > O_3 (8 W)/EC (8 W) (Table 1). The synergy coefficient between systems can be usefully quantified as the normalized difference between the rate constants of various conjunctive EC, UV/TiO_2 and ozone-related systems. A larger synergy coefficient indicates stronger promotion of the decolorization by the combined reaction systems. The synergy coefficients of the O_3 (8 W)/EC (8 W) and UV/TiO_2/O_3 (8 W) systems were −0.61 and −0.25, respectively. The combination of EC with O_3 and TiO_2 with UV/O_3 is suggested adversely to influence decolorization. In contrast, the synergy coefficients of UV/O_3 (8 W), UV/EC (8 W), UV/TiO_2/EC (8 W), UV/O_3 (8 W)/EC (8 W) and UV/TiO_2/O_3 (8 W)/EC (8 W) systems were 0.11, 0.15, 0.31, 0.04 and 0.07, respectively. The reasons for the promotion of decolorization by coupling UV with O_3, UV with EC and EC with UV/TiO_2 systems are explained above. Notably, UV/O_3 (8 W)/EC (8 W) accelerate decolorization to a rate higher than that achieved in the UV/O_3 (8 W) system; however, the O_3 (8 W)/EC (8 W) system is inhibitive, as compared with the O_3 (8 W) system. UV is more effective in the formation of hydroxyl radicals (Eqs. (7) and (9)) and UV light itself activates the bonds between dyes, causing further degradation; Fe^{2+} and O_3 lack this ability [16]. Fe^{2+} and Fe^{3+} can be produced by the EC method (Eqs. (10) and (14)); moreover, H_2O_2 is generated in the UV/O_3 system (Eq. (8)). Xu [6] indicated that the following reactions (Eqs. (29)–(31)) proceed when Fe^{2+}, Fe^{3+} and H_2O_2 are simultaneously present in a reactor. This result was similar to that obtained by combining UV/TiO_2 with EC, which may induce a Fenton or Fenton-like reaction and accelerate decolorization.

$$Fe^{3+} + H_2O + h\nu \rightarrow Fe^{2+} + H^+ + OH\bullet \quad (29)$$

$$Fe^{3+} + H_2O_2 \rightarrow Fe^{2+} + H^+ + HO_2\bullet \quad (30)$$

$$Fe^{2+} + H_2O_2 \rightarrow Fe^{3+} + OH^- + OH\bullet \quad (31)$$

Based on the above explanations, the promotional effect of the UV/O_3 (8 W)/EC (8 W) system was acceptable and reasonable. Moreover, Fe^{2+} and Fe^{3+} competed OH^- with O_3, reducing the yield of radicals according to Eqs. (3)–(5); hence, combining O_3 with EC adversely affects decolorization.

3.4. Analysis of energy consumption in EC, UV/TiO_2 and ozone-related systems

The efficiency of decolorization in conjunctive EC, UV/TiO_2 and ozone-related systems was examined. The results demonstrate that the combination of UV with O_3, UV with EC, and EC with UV/TiO_2 or UV/O_3 accelerated decolorization. The energy consumption in EC, UV/TiO_2 and ozone-related systems was further studied (Fig. 6). This work plots ln(C_o/C) against total energy consumption and determines the effective energy consumption constants (k_b). These values in conjunctive EC, UV/TiO_2 and ozone-related systems were found to be consistent

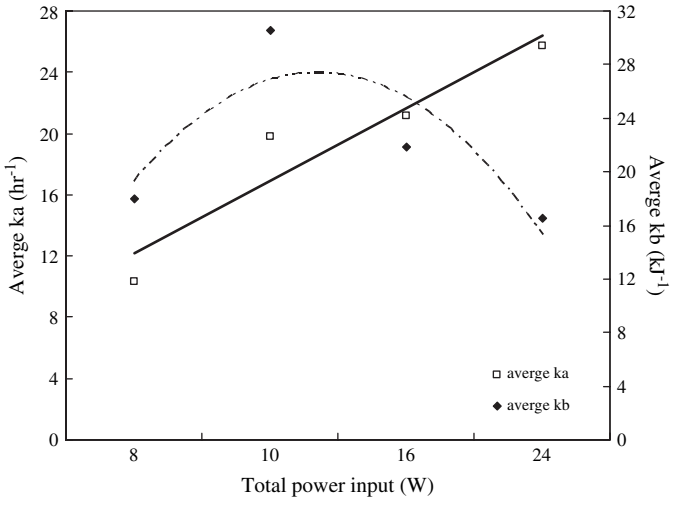

Fig. 7. Relationships among k_a, k_b and total input power in ozone-related systems.

with pseudo-first-order kinetics (Table 1). This investigation proposes that a higher k_b value corresponds to more efficient energy consumption during decolorization. The effective energy consumption constants follow the order O_3 (8 W) > UV/O_3 (8 W) > UV/TiO_2/O_3 (8 W) > UV/TiO_2/O_3 (8 W)/EC (8 W) ≧ UV/O_3 (8 W)/EC (8 W) > O_3 (8 W)/EC (8 W) (Table 1). Interestingly, the effective energy consumption constants did not increase in proportion to the total energy input. The results imply that not all of the input energy is used in decolorization. For simplicity, this research focused on ozone-related systems to evaluate the relationships among the reaction rate constant, the effective energy consumption constant and the total power input (Fig. 7). At total power inputs of 8, 10, 16 and 24 W, the average reaction rate constants of ozone-related systems were 10.4, 19.8, 21.2 and 25.7 h^{-1} and the effective energy consumption constants were 18.0, 30.6, 21.8 and 16.5 k/J, respectively. The mean reaction rate constants increased with the total power input; however, the effective energy consumption constants initially increased with total power input, and then declined. A favorable power input is suggested to maximize the efficiency of energy consumption. Although the reaction rate constant was not maximal, this work suggests that a total power input of 10–16 W can maximize the efficiency of energy consumption.

This investigation verified that the decolorization rate could be promoted by coupling UV with O_3, UV with EC, EC with UV/TiO_2 and EC with UV/O_3; however, all of the effective energy consumption constants of these systems dropped after coupling. The most effective total power input was 10–16 W, so this study suggests that UV/O_3 (8 W) and O_3 (16 W) systems were more effective and economic for dye decolorization than other single or coupled systems.

4. Conclusion

This work compares the decolorization efficiency and energy consumption of EC, UV/EC, UV/TiO_2, ozone, UV/ozone, ozone/EC, UV/TiO_2/ozone, UV/TiO_2/EC, UV/ozone/EC and UV/TiO_2/O_3/EC systems in terms of reaction rate constants and effective energy consumption constants. The k_a value of UV/O_3 (8 W) (17.94 h^{-1}) exceeded that of O_3 (8 W) (15.92 h^{-1}). The reaction rate constants of UV/TiO_2 and EC-related systems followed the order UV/TiO_2/EC (0.89 h^{-1}) > UV/TiO_2 (0.35 h^{-1}) > UV/EC (0.26 h^{-1}) ≧ EC (0.22 h^{-1}). The synergy coefficients of UV/O_3 (8 W), UV/EC (8 W), UV/TiO_2/EC (8 W), UV/O_3 (8 W)/EC (8 W) and UV/TiO_2/O_3 (8 W)/EC (8 W) systems were 0.11, 0.15, 0.31, 0.04 and 0.07, respectively. This study proposes that combining EC with UV/TiO_2 or UV/O_3 may induce a Fenton or Fenton-like reaction and accelerate decolorization. At a total power input of 8, 10, 16 and 24 W, the mean reaction rate constants of the ozone-related systems were 10.4, 19.8, 21.2 and 25.7 h^{-1} and the effective energy consumption constants were 18.0, 30.6, 21.8 and 16.5 k/J, respectively. This investigation suggests that a total power input of 10–16 W maximize the effectiveness of energy consumption, making the operation maximally economic.

Acknowledgements

The authors would like to thank the National Science Council of the Republic of China for financially supporting this research under Contract No. NSC 93-2621-Z-264-001.

References

[1] Kim TH, Park C, Shin EB, Kim S. Decolorization of disperse and reactive dyes by continuous electrocoagulation process. Desalination 2002;150:165–75.
[2] Daneshvar N, Ashassi-Sorkhabi H, Tizpar A. Decolorization of orange II by electrocoagulation method. Separation and Purification Technology 2003;31:153–62.
[3] Bayramoglu M, Kobya M, Can OT, Sozbir M. Operating cost analysis of electrocoagulation of textile dye wastewater. Separation and Purification Technology 2004;37:117–25.
[4] Mollah MYA, Pathak SR, Patil PK, Vayuvegula M, Agrawal TS, Gomes JAG, et al. Treatment of orange II azo-dye by electrocoagulation (EC) technique in a continuous flow cell using sacrificial iron electrodes. Journal of Hazardous Materials 2004;109:165–71.
[5] Golder AK, Hridata N, Samanta AN, Ray S. Electrocoagulation of methylene blue and eosin yellowish using mild steel electrodes. Journal of Hazardous Materials 2005;127:134–40.
[6] Xu Y. Comparative studies of the $Fe^{3+/2+}$–UV, H_2O_2–UV, TiO_2–UV–vis systems for the decolorization of a textile dye X-3B in water. Chemosphere 2001;43:1103–7.
[7] So CM, Cheng MY, Yu JC, Wong PK. Degradation of azo dye Procion Red MX-5B by photocatalytic oxidation. Chemosphere 2002;46:905–12.
[8] Hu C, Yu JC, Hao Z, Wong PK. Photocatalytic degradation of triazine-containing azo dyes in aqueous TiO_2 suspensions. Applied Catalysis B: Environmental 2003;42:47–55.
[9] Chen J, Liu M, Zhang J, Ying X, Jin L. Photocatalytic degradation of organic wastes by electrochemically assisted TiO_2 photocatalytic system. Journal of Environment Management 2004;70:43–7.
[10] Wu CH. Comparison of azo dye decolorization efficiency using UV/single semiconductor and UV/coupled semiconductor systems. Chemosphere 2004;57:601–8.
[11] Qamar M, Saquib M, Muneer M. Photocatalytic degradation of two selected dye derivatives, chromotrope 2B and amido black 10B, in aqueous suspensions of titanium dioxide. Dyes and Pigments 2005;65:1–9.
[12] Wu CH, Chang CL, Kuo CY. Decolorization of Amaranth by advanced oxidation processes. Reaction Kinetics and Catalysis Letters 2005;86:37–43.
[13] Wu CH, Chang CL. Decolorization of Procion Red MX-5B by advanced oxidation processes: comparative studies of the homogeneous and heterogeneous systems. Journal of Hazardous Materials 2006;128:265–72.
[14] Peyton GR, Glaze WH. The mechanism of photolytic ozonation. Abstract of Papers of the American Chemical Society 1985;189:5.
[15] Alaton IA, Balcioglu IA, Bahnemann DW. Advanced oxidation of a reactive dyebath effluent: comparison of O_3, H_2O_2/UV-C and TiO_2/UV-A processes. Water Research 2002;36:1143–54.
[16] Kurbus T, Marechal AML, Voncina DB. Comparison of H_2O_2/UV, H_2O_2/O_3 and H_2O_2/Fe^{2+} processes for the decolorisation of vinysulphone reactive dyes. Dyes and Pigments 2003;58:245–52.
[17] Tezcanli-Guyer G, Ince NH. Individual and combined effects of ultrasound ozone and UV irradiation: a case study with textile dyes. Ultrasonics 2004;42:603–9.
[18] Wang KH, Hsieh YH, Wu CH, Chang CY. The pH and anion effects on the heterogeneous photocatalytic degradation of *o*-methylbenzoic acid in TiO_2 aqueous suspension. Chemosphere 2000;40:389–94.
[19] Glaze WH, Kang JW, Chapin DH. The chemistry of water treatment processes involving ozone, hydrogen, and ultraviolet radiation. Ozone Science and Engineering 1987;9:335–52.
[20] Konsowa AH. Decolorization of wastewater containing direct dye by ozonation in a bath bubble column reactor. Desalination 2003;158:233–40.
[21] Koch M, Yediler A, Lienert D, Insel G, Kettrup A. Ozonation of hydrolyzed azo dye reactive yellow 84 (CI). Chemosphere 2002;46:109–13.

[22] Chu W, Ma CW. Quantitative prediction of direct and indirect dye ozonation kinetics. Water Research 2000;34:3153–60.
[23] Konstantinou IK, Albanis TA. TiO_2-assisted photocatalytic degradation of azo dyes in aqueous solution: kinetic and mechanistic investigations – a review. Applied Catalysis B: Environmental 2004;49:1–14.
[24] Mollah MYA, Schennach R, Parga JR, Cocke DL. Electrocoagulation – science and applications. Journal of Hazardous Materials 2001;84:29–41.
[25] Mrowetz M, Selli E. Effects of iron species in the photocatalytic degradation of an azo dye in TiO_2 aqueous suspensions. Journal of Photochemistry and Photobiology A: Chemistry 2004;162:89–95.
[26] Qu P, Zhao J, Shen T, Hidaka H. TiO_2-assisted photodegradation of dyes: a study of two competitive primary processes in the degradation of RB in an aqueous TiO_2 colloidal solution. Journal of Molecular Catalysis A: Chemical 1998;129:257–68.
[27] Chen Y, Sun Z, Yang Y, Ke Q. Heterogeneous photocatalytic oxidation of polyvinyl alcohol in water. Journal of Photochemistry and Photobiology A: Chemistry 2001;142:85–9.
[28] Stylidi M, Kondarides DI, Verykios XE. Pathways of solar light-induced photocatalytic degradation of azo dyes in aqueous TiO_2 suspensions. Applied Catalysis B: Environmental 2003;40:271–86.